Final Technical Report

DE-FG02-96ER20214

UNIVERSITY OF OKLAHOMA

PI: Michael J. McInerney 1996-2018

PI: Elizabeth A. Karr 2019-2024

Table of Contents

Introduction

This DOE Basic Energy Physical Biosciences project spanned a 28-year period and two project investigators. Numerous significant research discoveries have occurred over this time frame. Much of this work has been reported in peer-reviewed literature, with the publication of results from the last four years forthcoming. The overarching project themes have focused on probing the metabolism of syntrophic bacteria and their environments. Research supported by this project has been central to ten doctoral dissertations and one master's thesis at the University of Oklahoma [1-11]. The project has also supported numerous undergraduate research projects throughout the years. Additionally, several microbial genomes were sequenced and annotated in association with this work [12-16]. Key findings and publications from this work are highlighted. More detailed results are provided for unpublished and embargoed work. A complete list of publications and research products associated with this project is at the report's end [12-66].

Complete List of Publications, Theses, Dissertations, and Research Products Associated with this Project

1. Crable BR. Enzyme systems involved in interspecies hydrogen and formate transfer between syntrophic fatty and aromatic acid degraders and Methanospirillum hungatei. 2013;Dissertation - Doctor of Philosophy in Microbiology. https://shareok.org/handle/11244/7894.
2. DInh DM. Characterizing two enzymes involved in carbon utilization and energy production in *Syntrophus aciditrophicus* strain SB. 2022;Dissertation –Doctor of Philosophy in Microbiology https://shareok.org/handle/11244/336902.
3. Elshahed MS. Peripheral and central pathways involved in the biodegradation of monoaromatic compounds under anaerobic conditions. 2001;Dissertation - Doctor of Philosophy in Microbiology. https://shareok.org/handle/11244/335.
4. Jackson BE. Bioenergetic Perspectives of Syntrophic Substrate Degradation. 1999;Dissertation - Doctor of Philosophy in Microbiology. https://shareok.org/handle/11244/5863.
5. Le HM. Central Metabolic Pathways in the Syntrophic Metabolizer, *Syntrophus Aciditrophicus*. 2013;Thesis - Master of Science in Microbiology.
6. Losey NA. NADH-dependent, ferredoxin-independent hydrogen production in two model syntrophic bacteria. 2019;Dissertation - Doctor of Philosophy in Microbiology. https://shareok.org/handle/11244/319558.
7. Mouttaki H. Novel aspects of benzoate and crotonate metabolism by the strictly anaerobic bacterium *Syntrophus aciditrophicus* strain SB. 2007;Dissertation - Doctor of Philosophy in Microbiology. https://shareok.org/handle/11244/1250.
8. Sieber J. Investigations of interspecies transfer mechanisms important to syntrophic metabolism. 2011;Dissertation - Doctor of Philosophy in Botany and Microbiology. https://shareok.org/handle/11244/319167.
9. Struchtemeyer CG. Microorganisms from Anaerobic, Gas Condensate-Contaminated Sediments that Degrade Acetate, Butyrate, and Propionate Under

Methanogenic and Sulfate-reducing Conditions. 2009;Dissertation - Doctor of Philosophy in Microbiology. https://shareok.org/handle/11244/319156.
10. Thomas-James K. Enzymes involved in energy conservation via substrate-level phosphorylation in the syntrophic benzoate degrader, *Syntrophus aciditrophicus*. 2014;Dissertation - Doctor of Philosophy in Microbiology. https://shareok.org/handle/11244/10397.
11. Yaghoubi S. Biochemical insights into the unconventional approaches to energy conservation and electron transport in syntrophic metabolism. 2024;Dissertation – Doctor of Philosophy in Microbiology. https://shareok.org/handle/11244/340333.
12. Sieber JR, Sims DR, Han C, et al. The genome of *Syntrophomonas wolfei*: new insights into syntrophic metabolism and biohydrogen production. *Environ Microbiol.* 2010;12(8):2289-2301.
13. Callaghan AV, Morris BEL, Pereira IAC, et al. The genome sequence of *Desulfatibacillum alkenivorans* AK-01: a blueprint for anaerobic alkane oxidation. *Environmental Microbiology.* 2012;14(1):101-113.
14. McInerney MJ, Rohlin L, Mouttaki H, et al. The genome of *Syntrophus aciditrophicus*: life at the thermodynamic limit of microbial growth. *Proc Natl Acad Sci U S A.* 2007;104(18):7600-7605.
15. Plugge CM, Henstra AM, Worm P, et al. Complete genome sequence of *Syntrophobacter fumaroxidans* strain (MPOBT). *Stand Genomic Sci.* 2012;7:91-106 DOI:110.4056 /sigs.2996379.
16. Gunsalus RP, Cook LE, Crable B, et al. Complete genome sequence of *Methanospirillum hungatei* type strain JF1. *Stand Genomic Sci.* 2016;11:2-2.
17. Bhupathiraju VK, McInerney MJ, Woese CR, Tanner RS. *Haloanaerobium kushneri* sp nov., an obligately halophilic, anaerobic bacterium from an oil brine. *International Journal of Systematic Bacteriology.* 1999;49:953-960.
18. Coates JD, Bhupathiraju VK, Achenbach LA, McInerney MJ, Lovley DR. *Geobacter hydrogenophilus*, *Geobacter chapellei* and *Geobacter grbiciae*, three new, strictly anaerobic, dissimilatory Fe(III)-reducers. *International Journal of Systematic and Evolutionary Microbiology.* 2001;51:581-588.
19. Coates JD, Chakraborty R, McInerney MJ. Anaerobic benzene biodegradation - a new era. *Research in Microbiology.* 2002;153(10):621-628.
20. Coates JD, Cole KA, Michaelidou U, Patrick J, McInerney MJ, Achenbach LA. Biological control of hog waste odor through stimulated microbial Fe(III) reduction. *Appl Environ Microbiol.* 2005;71(8):4728-4735.
21. Crable BR, Plugge CM, McInerney MJ, Stams AJ. Formate formation and formate conversion in biological fuels production. *Enzyme Res.* 2011;2011:532536.
22. Crable BR, Sieber JR, Mao X, et al. Membrane complexes of *Syntrophomonas wolfei* involved in syntrophic butyrate degradation and hydrogen formation. *Front Microbiol.* 2016;7(1795).
23. Dinh DM, Thomas LM, Karr EA. Crystal structure of a putative 3-hydroxypimelyl-CoA dehydrogenase, Hcd1, from *Syntrophus aciditrophicus* strain SB at 1.78 A resolution. *Acta Cryst F.* 2023;79(6).
24. Elias DA, Suflita JM, McInerney MJ, Krumholz LR. Periplasmic cytochrome c(3) of *Desulfovibrio vulgaris* is directly involved in H-2-mediated metal but not sulfate reduction. *Appl Environ Microbiol.* 2004;70(1):413-420.

25. Elshahed M, Bhupathiraju V, Wofford N, Nanny M, McInerney M. Metabolism of benzoate, cyclohex-1-ene carboxylate, and cyclohexane carboxylate by *Syntrophus aciditrophicus* strain SB in syntrophic association with H_2-using microorganisms. *Appl Environ Microbiol.* 2001;67:1728-1738.
26. Elshahed MS, Gieg LM, McInerney MJ, Suflita JM. Signature metabolites attesting to the in situ attenuation of alkylbenzenes in anaerobic environments. *Environmental Science & Technology.* 2001;35(4):682-689.
27. Elshahed MS, McInerney MJ. Is interspecies hydrogen transfer needed for toluene degradation under sulfate-reducing conditions? *Fems Microbiology Ecology.* 2001;35(2):163-169.
28. Elshahed MS, McInerney MJ. Benzoate fermentation by the anaerobic bacterium *Syntrophus aciditrophicus* in the absence of hydrogen-using microorganisms. *Appl Environ Microbiol.* 2001;67(12):5520-5525.
29. Folmsbee M, Duncan K, Han SO, Nagle D, Jennings E, McInerney M. Re-identification of the halotolerant, biosurfactant-producing *Bacillus licheniformis* strain JF-2 as *Bacillus mojavensis* strain JF-2. *Syst Appl Microbiol.* 2006;29(8):645-649.
30. Folmsbee M, McInerney M, Nagle D. Anaerobic growth of *Bacillus mojavensis* and *Bacillus subtilis* requires deoxyribonucleosides or DNA. *Appl Environ Microbiol.* 2004;70(9):5252-5257.
31. Goudar CT, Harris SK, McInerney MJ, Suflita JM. Progress curve analysis for enzyme and microbial kinetic reactions using explicit solutions based on the Lambert *W* function. *Journal of Microbiological Methods.* 2004;59(3):317-326.
32. Hoehler T, Losey NA, Gunsalus RP, McInerney MJ. Environmental constraints that limit methanogenesis. In: Stams AJM, Sousa D, eds. *Biogenesis of Hydrocarbons.* Cham: Springer International Publishing; 2018:1-26.
33. Hotze EM, Le HM, Sieber JR, Bruxvoort C, McInerney MJ, Tweten RK. Identification and characterization of the first cholesterol-dependent cytolysins from Gram-negative bacteria. *Infect Immun.* 2013;81(1):216-225.
34. Jackson BE, Bhupathiraju VK, Tanner RS, Woese CR, McInerney MJ. *Syntrophus aciditrophicus* sp. nov., a new anaerobic bacterium that degrades fatty acids and benzoate in syntrophic association with hydrogen-using microorganisms. *Archives of Microbiology.* 1999;171(2):107-114.
35. Jackson BE, McInerney MJ. Thiosulfate disproportionation by *Desulfotomaculum thermobenzoicum*. *Appl Environ Microbiol.* 2000;66(8):3650-3653.
36. Jackson BE, McInerney MJ. Anaerobic microbial metabolism can proceed close to thermodynamic limits. *Nature.* 2002;415(6870):454-456.
37. James KL, Kung JW, Crable BR, et al. *Syntrophus aciditrophicus* uses the same enzymes in a reversible manner to degrade and synthesize aromatic and alicyclic acids. *Environ Microbiol.* 2019;21(5):1833-1846.
38. James KL, Ríos-Hernández LA, Wofford NQ, et al. Pyrophosphate-dependent ATP formation from acetyl coenzyme A in *Syntrophus aciditrophicus*, a new twist on ATP formation. *mBio.* 2016;7(4).
39. Kim M, Le HM, Xie X, et al. Two pathways for glutamate biosynthesis in the syntrophic bacterium *Syntrophus aciditrophicus*. *Appl Environ Microbiol.* 2015;81(24):8434.

40. Kim M, Le MH, McInerney MJ, Buckel W. Identification and characterization of Re-citrate synthase in *Syntrophus aciditrophicus*. *J Bacteriol 195:1689-1696.* 2013.
41. Kung JW, Seifert J, Boll M. Cyclohexane-1-carboxyl-coenzyme A (CoA) and cyclohex-1-ene-1-carboxyl-CoA dehydrogenases, two enzymes involved in the fermentation of benzoate and crotonate in *Syntrophus aciditrophicus*. *J Bacteriol.* 2013;195:3193-3200.
42. Li G, McInerney MJ. Use of Biosurfactants in Oil Recovery. In: Lee SY, ed. *Consequences of microbial interactions with hydrocarbons, oils, and lipids: production of fuels and chemicals.* Cham: Springer International Publishing; 2017:1-16.
43. Losey NA, Mus F, Peters JW, Le HM, McInerney MJ. *Syntrophomonas wolfei* uses an NADH-dependent, ferredoxin-independent [FeFe]-hydrogenase to reoxidize NADH. *Appl Environ Microbiol.* 2017;83(20):e01335-01317.
44. Marsh T, Leon N, McInerney M. Physiochemical factors affecting chromate reduction by aquifer materials. *Geomicrobiology Journal.* 2000;17(4):291-303.
45. Marsh T, McInerney M. Relationship of hydrogen bioavailability to chromate reduction in aquifer sediments. *Appl Environ Microbiol.* 2001;67(4):1517-1521.
46. McInerney M, Sieber J, Gunsalus R. Microbial sntrophy: ecosystem-level biochemical cooperation. *Microbe Magazine.* 2011;6:479-485.
47. McInerney M, Stams A, Boone D. Genus *Syntrophobacter*. In: Garrity GE-i-C, Brenner D, Krieg N, Staley J, eds. *Bergey's Manual of Systematic Bacteriology.* Vol 2nd Edition, Volume 2, The Proteobacteria. Baltimore, MD: Williams and Wilkins; 2005:1021-1027.
48. McInerney MJ. Listening to microbial conversations. *Microbial Biotechnology.* 2009;2(2):141-142.
49. McInerney MJ, Fink LD. Team-based learning enhances long-term retention and critical thinking in an undergraduate microbial physiology course. *Microbiology Education.* 2003;4:3-12.
50. McInerney MJ, Gieg LM. An overview of anaerobic metabolism. In: Nakano M, Zuber P, eds. *Strict and Facultative Anaerobes: Medical and Environmental Aspects.* Norfolk, U.K.: Horizon Scientific Press; 2004.
51. McInerney MJ, Hoehler T, Gunsalus RP, Schink B. Introduction to microbial hydrocarbon production: bioenergetics. In: Timmis KN, ed. *Handbook of Hydrocarbon and Lipid Microbiology.* Berlin, Heidelberg: Springer Berlin Heidelberg; 2010:319-335.
52. McInerney MJ, Sieber JR, Gunsalus RP. Syntrophy in anaerobic global carbon cycles. *Curr Opin Biotech.* 2009;20(6):623-632.
53. Mouttaki H, Nanny MA, McInerney MJ. Cyclohexane carboxylate and benzoate formation from crotonate in *Syntrophus aciditrophicus*. *Appl Environ Microbiol.* 2007;73(3):930-938.
54. Mouttaki H, Nanny MA, McInerney MJ. Metabolism of hydroxylated and fluorinated benzoates by *Syntrophus aciditrophicus* and detection of a fluorodiene metabolite. *Appl Environ Microbiol.* 2009;75(4):998-1004.
55. Peters F, Shinoda Y, McInerney MJ, Boll M. Cyclohex-1,5-diene-1-carbonyl-coenzyme A hydratases of *Geobacter metallireducens* and *Syntrophus*

aciditrophicus: evidence for a common benzoyl-CoA pathway in facultative and obligate anaerobes. *J Bacteriol.* 2007;189:1055-1060.
56. Sieber JR, Crable BR, Sheik CS, et al. Proteomic analysis reveals metabolic and regulatory systems involved in the syntrophic and axenic lifestyle of *Syntrophomonas wolfei*. *Front Microbiol.* 2015;6(115).
57. Sieber JR, Le HM, McInerney MJ. The importance of hydrogen and formate transfer for syntrophic fatty, aromatic and alicyclic metabolism. *Environ Microbiol.* 2014;16(1):177-188.
58. Sieber JR, McInerney MJ, Gunsalus RP. Genomic insights into syntrophy: the paradigm for anaerobic metabolic cooperation. *Ann Rev Microbiol.* 2012;66(1):429-452.
59. Sieber JR, McInerney MJ, Müller N, Schink B, Gunsalus RP, Plugge CM. Methanogens: syntrophic metabolism. In: Stams AJM, Sousa D, eds. *Biogenesis of Hydrocarbons.* Cham: Springer International Publishing; 2018:1-31.
60. Sousa DZ, Balk M, Alves M, et al. Degradation of long-chain fatty acids by sulfate-reducing and methanogenic communities. In: Timmis KN, ed. *Handbook of Hydrocarbon and Lipid Microbiology.* Berlin, Heidelberg: Springer Berlin Heidelberg; 2010:963-980.
61. Struchtemeyer C, Elshahed M, Duncan K, McInerney M. Evidence for aceticlastic methanogenesis in the presence of sulfate in a gas condensate-contaminated aquifer. *Appl Environ Microbiol.* 2005;71(9):5348-5353.
62. Struchtemeyer CG, Duncan KE, McInerney MJ. Evidence for syntrophic butyrate metabolism under sulfate-reducing conditions in a hydrocarbon-contaminated aquifer. *Fems Microbiology Ecology.* 2011;76(2):289-300.
63. Yaghoubi S, Arbing M, Gunsulas R, Karr EA. Crystal structure of the electron transfer flavoprotein EtfAB3 from *Syntrophomonas wolfeii*. *Target Journal: Acta Cryst F.* In Preparation.
64. Yaghoubi S, Dinh DM, Thomas LM, Wofford NQ, McInerney MJ, Karr EA. Functional and structural characterization of AMP-forming Acetyl-CoA synthetase (Acs1) from *Syntrophus aciditrophicus* strain SB. *Target journal: mBio.* In Preparation.
65. Thomas LM, Karr EA, Dinh DM. 3-oxoacyl-ACP reductase FabG. 2021;PDB ID 7SUB.
66. Thomas LM, Karr EA, Yaghoubi S, DInh DM. *Acetyl-CoA Synthetase (Acs1), Wild-type with Bound Acetyl-AMP from Syntrophous aciditrophicus.* 2024;PDB ID 94EP.

Genomes

Genome of *Syntrophus aciditrophicus*

The completed genome sequence of *Syntrophus aciditrophicus* SB, a model fatty- and aromatic acid-degrading syntrophic bacterium, provided the first glimpse of the composition and architecture of the electron transfer and energy-transducing systems needed to exist on marginal energy economies of a syntrophic lifestyle. The genome contained 3,179,300 base pairs and 3,169 genes, of which 51% (1,618 genes) were assigned putative functions. Genes with functional assignments were organized into pathways, and most biosynthetic pathways of a typical gram-negative organism were detected with several notable exceptions (e.g., the ability to synthesize 2-oxoglutarate). The genome content also suggests novel approaches to degrade fatty and aromatic acids that include multiple AMP-forming CoA ligases, as well as acyl-CoA synthetases. A distinctive feature of syntrophic metabolism is the need for reverse electron transfer, and the presence of a unique Rnf-type Na^+-translocating electron transfer complex, menaquinone, and membrane-bound Fe-S proteins suggests a mechanism to accomplish this task. The genome predicts multiple pyrophosphatases, Na^+-translocating ATP synthetases, a glutaconyl-CoA decarboxylase, and a formate cycle involving periplasmic and cytosolic formate dehydrogenases that suggest ways to form and dissipate ion gradients. Thus, *S. aciditrophicus,* although nutritionally self-sufficient, appears to be a syntrophic specialist with limited fermentative and respiratory metabolism. The genome sequence of *S. aciditrophicus* SB reveals the essential features required for growth with fatty and aromatic acids by a syntrophic lifestyle.

- McInerney MJ, Rohlin L, Mouttaki H, et al. The genome of *Syntrophus aciditrophicus*: life at the thermodynamic limit of microbial growth. *Proc Natl Acad Sci U S A.* 2007;104(18):7600-7605.

Genome of *Syntrophomonas wolfei*

We completed the manual annotation of the *Syntrophomonas wolfei* genome. *S. wolfei,* other sequenced syntrophic metabolizers, and thermophilic anaerobes known to produce high molar ratios of hydrogen from glucose have genes to produce H_2 from NADH by an electron bifurcation mechanism. Comparative genomic analysis also suggests that formate production from NADH may involve electron bifurcation. However, further biochemical characterization of two NADH-dependent hydrogenase showed that these enzymes were ferredoxin-independent and not electron bifurcating as discussed more fully later in this report. A membrane-bound, iron-sulfur oxidoreductase found in *S. wolfei* and *Syntrophus aciditrophicus* may uniquely involve reverse electron transfer during syntrophic fatty acid metabolism.

- Sieber JR, Sims DR, Han C, et al. The genome of *Syntrophomonas wolfei*: new insights into syntrophic metabolism and biohydrogen production. *Environ Microbiol.* 2010;12(8):2289-2301.

Genome of *Methanospirillum hungatei* JF-1

M. hungatei is the near-ubiquitous partner organism in syntrophic partnerships. The first sequenced genome in the family *Methanospirillaceae*, the circular genome is 3.5 Mb and contains 3,239 protein-coding and 68 RNA genes. With a relatively large genome for a hydrogenotrophic and formate-using methanogen, suggesting its genome may provide insight into its unique partnering capabilities with syntrophs.

- Gunsalus RP, Cook LE, Crable B, et al. Complete genome sequence of *Methanospirillum hungatei* type strain JF1. *Standards in genomic sciences.* 2016;11:2-2.

Insights into Syntrophic Metabolism

A new syntroph

A new, strictly anaerobic, gram-negative, non-motile, non-spore-forming, rod-shaped bacterium that degrades benzoate and certain fatty acids in syntrophic association with hydrogen/formate-using microorganisms, Strain SB^T, was identified. The DNA base composition of strain SB^T was 43.1 mol % G + C. Analysis of the 16S rRNA gene sequence placed strain SB^T in the delta subdivision of the Proteobacteria, with sulfate-reducing bacteria. Strain SB^T was most closely related to members of the genus *Syntrophus*. The clear phenotypic and genotypic differences between strain SB^T and the two described species in the genus *Syntrophus* justified the formation of a new species, *Syntrophus aciditrophicus.*

- Jackson BE, Bhupathiraju VK, Tanner RS, Woese CR, McInerney MJ. *Syntrophus aciditrophicus* sp. nov., a new anaerobic bacterium that degrades fatty acids and benzoate in syntrophic association with hydrogen-using microorganisms. *Archives of Microbiology.* 1999;171(2):107-114.

Syntrophic metabolism

We discovered that *S. aciditrophicus* forms benzoate and cyclohexane-1-carboxylate from crotonate and elucidated the main metabolic steps in the pathway. Cyclohexane-1-carboxylate formation represents one of the few cases in biology where a saturated ring compound is made from a straight- chain organic acid. The pathway for cyclohexane-1-carboxylate from crotonate appears to be a reversal of the benzoate degradation pathway. This suggests that the direction of metabolism is controlled by thermodynamic regimes and operates at high efficiency. We discovered that benzoate is respired by *S. aciditrophicus*. The increase in molar growth yield with crotonate and benzoate and the

formation of [ring-^{13}C]-cyclohexane- 1- carboxylate from [ring-^{13}C]-benzoate in the presence of crotonate are consistent with benzoate serving as an electron acceptor. Diverse fates for benzoate metabolism exist in methanogenic environments including syntrophic metabolism, fermentation, and respiration.

Many fermentative bacteria obtain energy for growth by reactions where the free energy change is less than that needed to synthesize ATP. Yet, these bacteria directly couple substrate metabolism to ATP synthesis by classical phosphoryl transfer reactions. To explain the energy economy of these organisms, it has been proposed that biological systems conserve energy in discrete amounts with a minimum biochemically convertible energy value of approximately –20 kJ/mol. This concept predicts that anaerobic substrate decay ceases before the minimum free energy value is reached as several studies indicate. We showed that metabolism by syntrophic associations, those where the degradation of a substrate by one species is thermodynamically possible only by end product removal by another species, can occur at values close to thermodynamic equilibrium ($\Delta G' \sim 0$ kJ/mol). The free energy remaining when substrate metabolism halts is not constant. It depends on the terminal electron-accepting reaction and the amount of energy required for substrate activation. The observation that syntrophic associations can metabolize near thermodynamic equilibrium indicates that bacteria operate astoundingly efficient catabolic systems.

Our experimental observations imply that syntrophically metabolizing bacteria may maximize energy conservation when thermodynamic constraints begin to limit substrate degradation, possibly by altering their phosphorylation potential or electromotive membrane potential in response to signals from their hydrogen-using partner. Our results indicate that the free energy remaining when metabolism stops is highly variable and imply that the extent of metabolism depends upon the activation steps used for substrate metabolism as well as the terminal electron-accepting condition. Collectively, these data show that a universal minimum free energy does not predict the extent of substrate metabolism and that bacterial metabolism can proceed near thermodynamic equilibrium, a condition that is often thought to be a biological improbability.

- Elshahed M, Bhupathiraju V, Wofford N, Nanny M, McInerney M. Metabolism of benzoate, cyclohex-1-ene carboxylate, and cyclohexane carboxylate by *Syntrophus aciditrophicus* strain SB in syntrophic association with H_2-using microorganisms. *Appl Environ Microbiol.* 2001;67:1728-1738.

- Elshahed MS, McInerney MJ. Benzoate fermentation by the anaerobic bacterium *Syntrophus aciditrophicus* in the absence of hydrogen-using microorganisms. *Appl Environ Microbiol.* 2001;67(12):5520-5525.

- Jackson BE, McInerney MJ. Anaerobic microbial metabolism can proceed close to thermodynamic limits. *Nature.* 2002;415(6870):454-456.

- McInerney MJ, Rohlin L, Mouttaki H, et al. The genome of *Syntrophus aciditrophicus*: life at the thermodynamic limit of microbial growth. *Proc Natl Acad Sci U S A.* 2007;104(18):7600-7605.

- Mouttaki H, Nanny MA, McInerney MJ. Cyclohexane carboxylate and benzoate formation from crotonate in *Syntrophus aciditrophicus*. *Appl Environ Microbiol.* 2007;73(3):930-938.

- Peters F, Shinoda Y, McInerney MJ, Boll M. Cyclohex-1,5-diene-1-carbonyl-coenzyme A hydratases of *Geobacter metallireducens* and *Syntrophus aciditrophicus*: evidence for a common benzoyl-CoA pathway in facultative and obligate anaerobes. *J Bacteriol.* 2007;189:1055-1060.

- Jackson BE. Bioenergetic Perspectives of Syntrophic Substrate Degradation. 1999; Dissertation - Doctor of Philosophy in Microbiology. https://shareok.org/handle/11244/5863.

We detected a new membrane-bound complex in *S.wolfei* involved in reverse electron transfer during syntrophic growth with butyrate. The complex was not detected when *S. wolfei* grew syntrophically with crotonate, a compound that does not require reverse electron transfer for its metabolism, or axenically with crotonate. Mass spectrometry detected unique peptides of the membrane-bound, iron-sulfur oxidoreductase, the beta subunit of electron transfer flavoprotein, and two subunits of a membrane-bound hydrogenase were detected. These data support the conclusion that a novel membrane complex forms hydrogen from electrons generated during beta-oxidation.

A combination of genomic analysis, gene expression, enzymatic analyses, and inhibitor-based approaches were used to determine the importance of H_2 and/or formate transfer for syntrophic benzoate and cyclohexane-1- carboxylate metabolism by *S. aciditrophicus* and syntrophic butyrate oxidation by *S. wolfei. S. wolfei* expressed all three hydrogenase gene systems and two of five formate dehydrogenase gene systems when grown syntrophically on butyrate. Butyrate metabolism and CH_4 production by washed cell suspensions of *S. wolfe*i and the methanogen were inhibited by hydrogenase inhibitors, cyanide, and carbon monoxide but not by the formate dehydrogenase inhibitor, hypophosphite. Genes for one hydrogenase and two formate dehydrogenases were induced when *S. aciditrophicus* grew syntrophically on benzoate or cyclohexane-1-carboxylate. Syntrophic benzoate oxidation and CH_4 production were inhibited by hypophosphite but not cyanide and carbon monoxide. All three inhibitors were equally effective in halting syntrophic cyclohexane-1-carboxylate oxidation. These results demonstrate that syntrophic fatty, alicyclic, and aromatic acid metabolism involves H_2 or formate transfer rather than direct electron transfer by nanowires. Secondly, the importance of H_2 versus formate transfer depends on the substrate and organism involved.

We determined the membrane protein complexes in two phylogenetically related syntrophic microorganisms: the aromatic and fatty acid oxidizer, *Syntrophus aciditrophicus*, and the propionate-oxidizing bacterium, *Syntrophobacter fumaroxidans*. We detected peptides for ATP synthase, NADH:ferredoxin oxidoreductase, pyrophosphatase, and others. Interestingly, contrary to our prediction, the NADH:ferredoxin oxidoreductase peptides were only detected in *S. aciditrophicus*

cultures grown under conditions not requiring reverse electron transfer. NADH:ferredoxin oxidoreductase peptides were not detected in *S. fumaroxidans*.

We delineated the major conduit for electron flow from butyryl-CoA to hydrogen and formate in *S. wolfei*, which involves a membrane-bound FeS oxidoreductase and a hydrogenase (Hyd2). In *S. aciditrophicus*, we showed that Rnf catalyzes the energetically unfavorable reduction of viologen dyes with NADH. Quantitative real time-polymerase chain reaction and proteomic studies provided strong evidence for the involvement of these enzyme systems in syntrophic metabolism.

- Plugge CM, Henstra AM, Worm P, et al. Complete genome sequence of *Syntrophobacter fumaroxidans* strain (MPOBT). Stand Genomic Sci. 2012;7:91-106 DOI:110.4056 /sigs.2996379.
- Sieber JR, Crable BR, Sheik CS, et al. Proteomic analysis reveals metabolic and regulatory systems involved in the syntrophic and axenic lifestyle of *Syntrophomonas wolfei*. *Front Microbiol.* 2015;6(115).
- Crable BR, Sieber JR, Mao X, et al. Membrane complexes of *Syntrophomonas wolfei* involved in syntrophic butyrate degradation and hydrogen formation. *Front Microbiol.* 2016;7(1795).
- Gunsalus RP, Cook LE, Crable B, et al. Complete genome sequence of *Methanospirillum hungatei* type strain JF1. *Standards in genomic sciences.* 2016;11:2-2.

We identified and characterized one of the main enzymes involved in NADH cycling in *S. wolfei*, the Fe-Fe hydrogenase, Hyd1 (encoded by Swol_1017-1019). *hyd1* was cloned and heterologously expressed, and its gene product was characterized. Hyd1 oxidized NADH and reduced NAD+ without the presence of ferredoxin. The presence of oxidized ferredoxin did not accelerate the rate of NAD+ reduction nor did the presence of reduced ferredoxin increase the rate of hydrogen production from NADH as is reported for confurcating Fe-Fe hydrogenases. These results suggest that Hyd1 is a NADH-dependent Fe-Fe hydrogenase but not a confurcating hydrogenase, i.e., one that uses reduced ferredoxin to drive the unfavorable production of hydrogen from NADH. NADH-dependent, ferredoxing-independent hydrogenases require low hydrogen partial pressures for continued hydrogen production. The use of non-electron bifurcating hydrogenase by syntrophic metabolizers explains, in part, the need for a hydrogen-using microbe such as a methanogen.

- Losey NA, Mus F, Peters JW, Le HM, McInerney MJ. *Syntrophomonas wolfei* uses an NADH-dependent, ferredoxin-independent [FeFe]-hydrogenase to reoxidize NADH. *Appl Environ Microbiol.* 2017;83(20):e01335-01317.

Use of reversible enzyme pathways in degradation and synthesis of aromatic and alicyclic acids in *S. aciditrophicus*

Stable isotope analyses showed the incorporation of ^{13}C from 1-^{13}C-labeled acetate into crotonate, benzoate, and cyclohexane-1-carboxylate during the degradation of these substrates. Thus, syntrophic metabolism involves reversible enzyme systems that operate close to thermodynamic equilibrium but conserve energy in a highly efficient manner.

- James KL, Kung JW, Crable BR, et al. *Syntrophus aciditrophicus* uses the same enzymes in a reversible manner to degrade and synthesize aromatic and alicyclic acids. *Environ Microbiol.* 2019;21(5):1833-1846.

Glutamate Biosynthesis in *S. aciditrophicus*

The isotopomer profiling and ^{13}C-NMR spectroscopy showed that *S. aciditrophicus* synthesizes glutamate by two pathways. The minor route involved the use of re-citrate synthase (30-40%), whereas the majority of glutamate was synthesized via the reductive carboxylation of succinate. *S. aciditrophicus* is the second example of a microbial species to employ two pathways for glutamate synthesis.

- Kim M, Le MH, McInerney MJ, Buckel W. Identification and characterization of Re-citrate synthase in *Syntrophus aciditrophicus*. *J Bacteriol 195:1689-1696.* 2013.
- Kim M, Le HM, Xie X, et al. Two Pathways for Glutamate Biosynthesis in the Syntrophic Bacterium *Syntrophus aciditrophicus*. *Appl Environ Microbiol.* 2015;81(24):8434.

Novel mechanism for ATP synthesis in *S. aciditrophicus*

We found that *S. aciditrophicus* uses a novel mechanism for ATP from acetyl-CoA. This specialized bacterium uses pyrophosphate, an important prebiotic energy source, and the AMP-forming, acetyl-CoA synthetase (Acs1) to produce ATP. *S. aciditrophicus* uses AMP-forming, acyl-CoA synthetases to activate benzoate, cyclohexane-1-carboxylate, and crotonate to their respective coenzyme A (CoA) derivatives. The pyrophosphate formed during substrate activation can then be used by Acs1 to produce ATP, indicating the importance of pyrophosphate cycling in *S. aciditrophicus*.

S. aciditrophicus maintains a very low energy charge (0.24 ± 0.04) compared to other bacteria, such as *Escherichia coli*, which has an energy charge of 0.93 ± 0.005. The low energy charge suggests that the free energy for ATP formation (free energy of phosphorylation) may also be low, allowing syntrophic bacteria to use reactions with low free energy changes such as Acs1.

- James KL, Ríos-Hernández LA, Wofford NQ, et al. Pyrophosphate-dependent ATP formation from acetyl coenzyme A in *Syntrophus aciditrophicus*, a new twist on ATP formation. *mBio.* 2016;7(4).

Structural and Functional Characterization of *Sa*Acs1

We obtained two distinct crystal morphologies of *Sa*Acs1 (**Fig 1 A & B**). The crystal in **Fig 1A** contained no ligands and resulted in a 2.6 Å apo structure solution (**Fig 1C, red**) lacking the CTD of the enzyme *Sa*Acs1ND. The needle-like crystals in **Fig 4B** were co-crystalized with ATP and acetate. From these needle-like crystals, we have obtained two full-length structural solutions (3.4 Å, *Sa*Acs1$^{3.4,}$ and 2.2 Å, *Sa*Acs1$^{2.2}$, **Fig 4C**, blue and cyan, respectively), both containing acetyl-AMP in the active site.

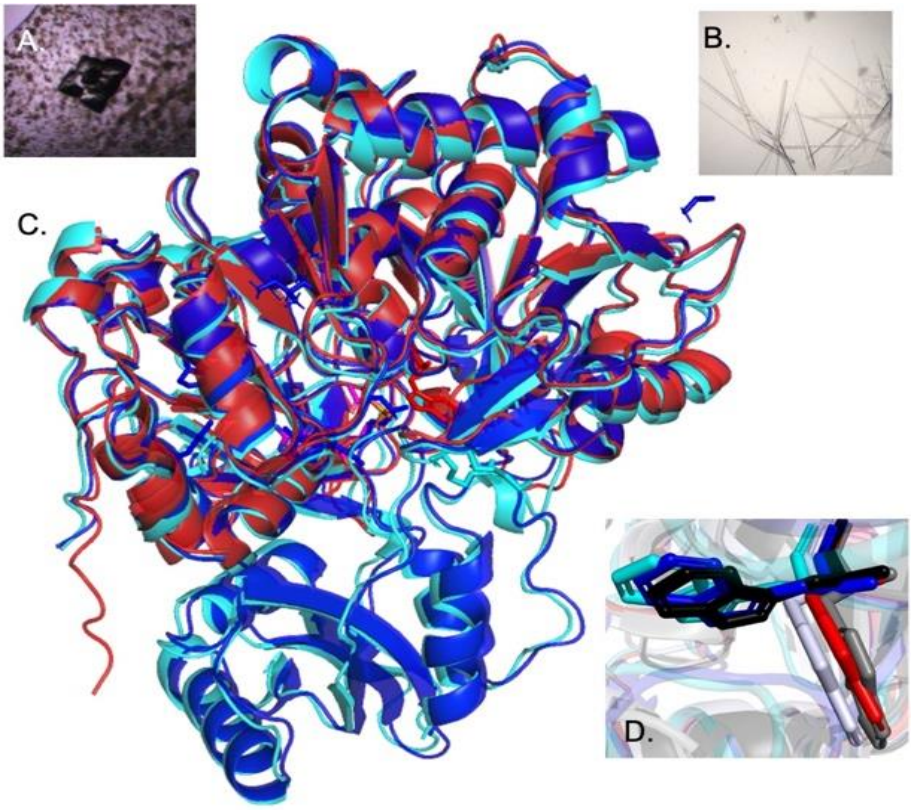

Figure 1. The two crystals morphologies observed for *Sa*Acs1 (A and B). (C) Overlay of three *Sa*Acs1 structures obtained. *Sa*Acs1–2.2Å (cyan), *Sa*Acs1–3.4Å (blue), *Sa*Acs1-ND 2.6Å (red). (D) The position of the tryptophan in the CoA tunnel for the three SaAcs1 structures–2.2Å (cyan), 3.4Å (blue), ND–2.6Å (red) compared to *Cn*Acs in its three conformations (AD, black; TE, dark gray; pre-active, silver).

Figure 2 shows the active site's ATP/acetyl-AMP/AMP pocket and the residues directly interacting via hydrogen bonds. G395 and T420 stabilize the adenine ring of the acetyl-AMP. Several other residues interact with the acetyl-AMP in *Sa*Acs1, which is consistent with interactions seen in other Acs-family structures. Overall, the acetyl-AMP binding pocket is conserved, although K619 protrudes further into the binding pocket than what is seen for other Acs structures.

At the opening of the CoA binding pocket, there is a conserved CoA loop that contains two highly conserved positively charged amino acids that are known to interact with the nucleotide end of the CoA molecule in other Acs structures (**Fig 3A**). Nevertheless, in all Acs structures available in the PDB (19 in total), the relative positions of these two side chains and the CoA loop containing a two-stranded anti-parallel beta-sheet are conserved. The CoA loop nor the side chain positions vary regardless of the conformation or whether CoA is bound. The residues are positioned so that the arginine (**Fig 3B**- ex *Se* R191) interacts with the adenine ring, and the R/K (**Fig 3B**- ex *Se* R194) interacts with the phosphate on the 3' carbon of the ribose of CoA, respectively. However, the corresponding residues and CoA loop in *Sa*Acs1 (R199 and K202, respectively; **Fig 3 B, C**) are shifted compared to other Acs structures. Additionally, the two strands of the beta-sheet within the CoA loop are extended in the *Sa*Acs1 structure compared to others. **Figure 3B** provides an illustrative sampling of structures in the two active conformations (thioester-forming PDB IDs 7L4G-C, 2P2F; adenylate-forming PDB IDs 1RY2, 74LG-B) with (PDB ID 2P2F, PDB ID 5K85) and without (PDB IDs 7L4G-C, 7L4G-B, 1RY2) CoA bound compared to *Sa*Acs1. Additionally, the shifted position of the CoA loop is maintained in all three *Sa*Acs1 structures we have obtained

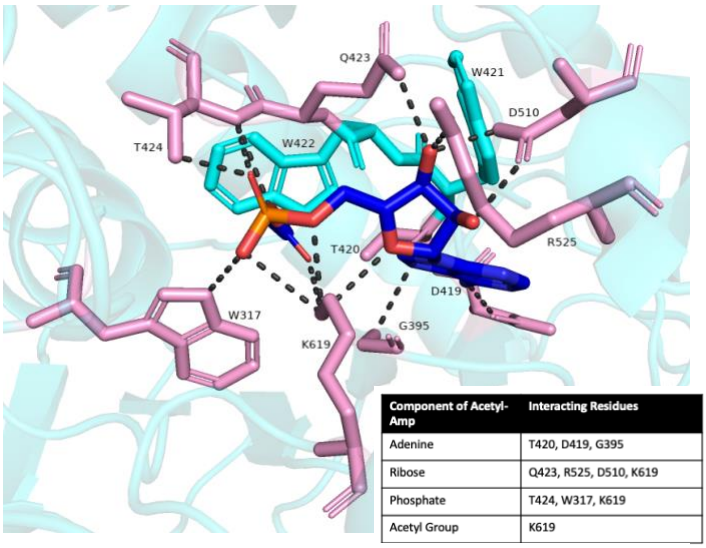

Component of Acetyl-Amp	Interacting Residues
Adenine	T420, D419, G395
Ribose	Q423, R525, D510, K619
Phosphate	T424, W317, K619
Acetyl Group	K619

Figure 2. Acetyl-AMP (blue) in the active site of the 2.2 Å structure of *Sa*Acs1 (cyan). The side chains of W421 and W422 are shown in cyan. The amino acids that interact directly with the acetyl-AMP are shown in pink and listed on the inset table.

(**Fig 3C**). We hypothesized that the shifted CoA loop is integral to the propensity of *Sa*Acs1 to operate in the ATP/acetate-forming direction.

A glutamic acid followed by a glycine residue leading into the loop region are highly conserved in most Acs proteins/structures. However, in *Sa*Acs1, these are replaced with glycine and threonine (**Fig 3A**). To determine the impact of these residues on the

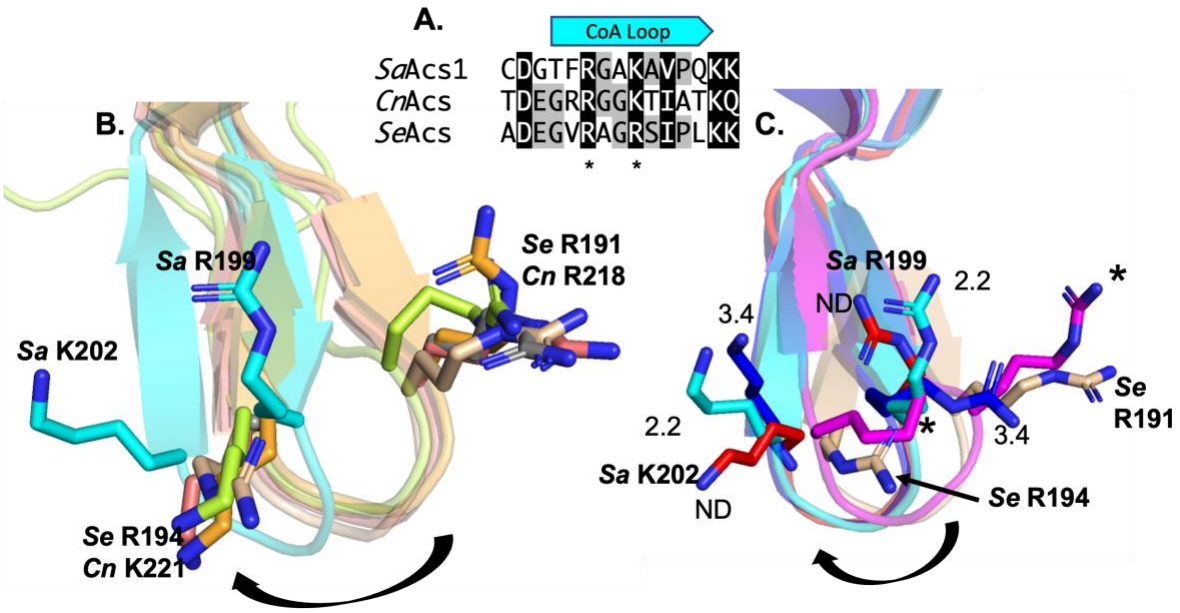

Figure 3. CoA loop of Acs-family proteins. (A). Amino acid alignment of the CoA loop region of the *Sa*, *Cn* and *Se* Acs proteins. Amino acids shaded in black share high identity. The asterisks indicate the residues within the loop (*Cn* R218, K221 and *Se* R191, R194) that are known to be important in binding/function and are shifted in the *Sa*Acs1 (*Sa* R199, K202) structure. (B) Structural alignment of the CoA loop of Acs structures in both the AD and TE conformations with and without CoA bound compared to *Sa*Acs1 (cyan) with the arginine and arginine/lysine side chains shown – *Se*Acs PDB ID 2P2F in TE-conformation with CoA, tan; *Sc*Acs PDB 1RY2 AD-conformation without CoA, lime; *Cn*Acs PDB ID 7L4G chain C TE-conformation without CoA, rose, and chain B AD-conformation without CoA, orange, PDB ID 5K85 TE-conformation with CoA, dark gray (C) Structural overlay of the CoA loop of the four *Sa*Acs1 structures [2.2 Å (cyan), 3.4 Å (blue), ND (red), and G196E/T197T variant (2.2 Å, magenta)] compared to the CoA loop of *Se*Acs (tan).

positioning of this loop, we generated a variant shifting the residues back to the conserved glutamic acid/glycine pair, *Sa*Acs1$^{G196E/T197G}$. A structure of the *Sa*Acs1$^{G196E/T197G}$ variant (2.4 Å, AD-conformation) shows that the loop position has shifted closer to that noted in other Acs-family proteins (**Fig 3C, magenta**). Notably, additional residues that interact with this end of the CoA molecule are in the CTD (*Sa*Acs R594/*Se*Acs R584) and thus are located remote from the CoA pocket in the adenylate-forming conformation of the enzyme. However, rotation of the C-terminal domain of *Sa*Acs1 at the hinge reside (D527) using the TE-conformations of the *Se* and *Cn* Acs structures as a guide allows for an approximation and, in conjunction with initial kinetic data has allowed us to propose

additional hypotheses for residues involved in acetyl-CoA binding when the enzyme is operating in the ATP-forming direction.

Our earlier data indicated that *Sa*Acs1 operates in the ATP-forming direction *in vitro* and that *in vivo,* high concentrations of pyrophosphate and AMP likely contribute to the overall operation in the ATP-forming direction as its primary cellular role. Until our recent studies, functional characterization of other Acs proteins has focused on the direction of the AMP-forming reaction. Therefore, no experimental data probed their ability/propensity to operate in the ATP-forming direction *in vitro.* Our structural characterization shows key differences between *Sa*Acs1 and other Acs family proteins in a highly conserved CoA loop region (**Fig 3**). To formally test the hypothesis that these structural differences contribute to the propensity of *Sa*Acs1 to operate in the ATP-forming direction, we used recombinant *Cryptococcus neoformans* (*Cn*) and *Salmonella enterica (Se)* Acs expressed from the same expression constructs as *Sa*Acs1 to ensure that any impact that the tag had on activity was consistent across the proteins, (*Se*Acs ^{C5AA6XHis} and *Cn*Acs^{C5AA6XHis}).

Table 1. Acs Kinetic Data for AMP and ATP substrates

Reaction Direction	AMP-Forming (forward)			ATP-Forming (reverse)		
Limiting Substrate	ATP			AMP		
	K_M (μM)	k_{cat} (s^{-1})	k_{cat}/K_M ($\mu M^{-1}\ s^{-1}$)	K_M (μM)	k_{cat} (s^{-1})	k_{cat}/K_M ($\mu M^{-1} s^{-1}$)
*Sa*Acs1^{WT}	303.6 ± 48.37	121.7 ± 3.59	0.4 ± 0.07	102.5 ± 27.33	101.6 ± 4.91	0.99 ± 0.18
SeAcs	93.5 ± 20.73	86.08 ± 3.76	0.92 ± 0.18	176.6 ± 51.81	74.45 ± 4.84	0.42 ± 0.09
CnAcs	139.8 ± 24.58	105.4 ± 3.46	0.75 ± 0.14	171.9 ± 42.22	116.6 ± 7.04	0.68 ± 0.17
*Sa*Acs1$^{G196E/T197G}$	159.2 ± 39.61	73.63 ± 3.24	0.46 ± 0.14	163.7 ± 35.66	54.66 ± 2.48	0.33 ± 0.07

*Sa*Acs1 had a much higher K_M (e.g., lower affinity) for ATP than either *Se* or *Cn*Acs (**Table 1**, AMP-forming reaction direction). The resulting k_{cat}/K_M in the forward/AMP-forming reaction direction were ~1.9 to 2.3-fold higher for *Cn* and *Se*Acs, respectively. For the other two forward reaction substrates (acetate and CoA), *Sa*Acs1 has a higher K_M than *Se*Acs1 but is lower than *Cn*Acs. However, the k_{cat}/K_M was similar for all three enzymes when these two substrates were limiting (data not shown for acetate and CoA). For the reverse reaction (ATP-forming direction), *Sa*Acs1 had a higher affinity (lower K_M) for all three of the substrates [AMP (**Table 1**), acetyl-CoA, and PP_i (not shown)] compared to *Cn* and *Se* Acs. The values for k_{cat}/K_M were inverse to what was seen in the forward reaction direction. These data confirm that *Sa*Acs1 has a higher affinity for the substrates (AMP, acetyl-CoA, PP_i) of the reverse reaction (ATP-forming direction) than Acs-family members *Cn* and *Se* Acs. Additionally, the catalytic efficiency of *Sa*Acs1 is greater in the direction of ATP formation. We hypothesized that the enhanced turnover efficiency of *Sa*Acs1

(compared to *Cn* and *Se*Acs) when acetyl-CoA is limiting is attributed to the shifted CoA loop and residues that contact the nucleotide end of the molecule that would better accommodate entry and catalysis of the larger acetyl-CoA molecule.

The structure of our *Sa*Acs1$^{G196E/T197G}$ variant showed that the CoA loop shifted in *Sa*Acs1 compared to other Acs-family proteins is partially restored (**Fig 3C**). Therefore, we performed kinetic assays with *Sa*Acs1$^{G196E/T197G}$ to determine how these structural changes impacted activity. In the variant, the affinity for ATP (forward reaction direction, **Table 2**) is increased, and the affinity for AMP (reverse reaction direction, **Table 1**) decreases. The catalytic efficiency decreases in both directions, but the k_{cat}/K_M for the reverse reaction looks closer to that of *Se*Acs than *Sa*Acs1^{WT}(**Table 1**). Similar trends were seen for acetyl-CoA and PP_i (data not shown). This further supported our hypothesis that the shifted CoA loop contributes to the propensity of *Sa*Acs1 to operate in the reverse direction.

In other Acs structures, the residues corresponding to R199 and K202 are shown to interact with the nucleotide end of the CoA molecule. Given the shifted CoA loop position, the R-group of K202 is rotated away from the CoA pocket (~7.5 to 10 Å compared to the corresponding residue in other structures), and R199 sits at that position (**Fig 3B**). Therefore, we constructed two initial variants, *Sa*Acs1^{R199A} and *Sa*Acs^{K202A}, at these positions for preliminary insight into whether the R groups of these residues are likely directly involved in binding CoA or acetyl-CoA (depending on reaction direction) or forming interactions that stabilize the nucleotide interface. *Sa*Acs1^{R199A} and *Sa*Acs^{K202A} were inactive in the ATP-forming direction but maintained activity in the AMP-forming direction. *Sa*Acs1^{R199A} behaved similarly to the *Se*Acs^{R194A} (based on amino acid alignments, this corresponds to position K202 in *Sa*Acs1) with an increased K_M for ATP and a decreased K_M for CoA. This is unsurprising given that these residues overlay each other (**Fig 3B**). However, *Sa*Acs^{K202A} had an increased K_M (lower affinity) for both ATP and CoA (in the forward direction) compared to *Sa*Acs^{WT}. These data showed that these two residues are critical for the alignment of acetyl-CoA in the active site in the first reaction step in the ATP-forming direction and that these two residues play slightly different roles in CoA binding in the second reaction step in the AMP-forming direction than what is seen for other Acs-family proteins.

A full report of several SaAcs1 wild-type and variant structures and their enzymatic activities is forthcoming.

- DInh DM. Characterizing two enzymes involved in carbon utilization and energy production in *Syntrophus aciditrophicus* strain SB. 2022; Dissertation –Doctor of Philosophy in Microbiology https://shareok.org/handle/11244/336902.

- Yaghoubi S, Dinh DM, Thomas LM, Wofford NQ, McInerney MJ, Karr EA. Functional and Structural Characterization of AMP-forming Acetyl-CoA Synthetase (Acs1) from *Syntrophus aciditrophicus* strain SB. *Target journal: mBio.* In Preparation.

- Yaghoubi S. Biochemical insights into the unconventional approaches to energy conservation and electron transport in syntrophic metabolism. 2024; Dissertation – Doctor of Philosophy in Microbiology. https://shareok.org/handle/11244/340333.

- Thomas LM, Karr EA, Yaghoubi S, DInh DM. Acetyl-CoA Synthetase (Acs1), Wild-type with Bound Acetyl-AMP from *Syntrophous aciditrophicus.* 2024; PDB ID 94EP.

Crystal structure of Hcd1, from *Syntrophus aciditrophicus*

The crystallized apo-*Sa*Hcd1 was resolved to 1.78 Å, with notable features such as a NAD(P)-binding Rossmann-like domain typical of short-chain dehydrogenase/reductase (SDR) proteins. Structurally, *Sa*Hcd1 exhibited key variations from similar SDR proteins, particularly in regions associated with cofactor binding. Unique structural differences included a shifted 310/α-helix and altered positions of helices and loops. Sequence analysis confirmed the presence of a glycine-rich TGXXXGXG motif, typically involved in NADPH binding, though some structural elements suggest *Sa*Hcd1 might also interact with NAD+/NADH. In its functional form, *Sa*Hcd1 appears to form a dimer, as indicated by size-exclusion chromatography and PISA analysis.

- DInh DM. Characterizing two enzymes involved in carbon utilization and energy production in *Syntrophus aciditrophicus* strain SB. 2022; Dissertation – Doctor of Philosophy in Microbiology https://shareok.org/handle/11244/336902.
- Dinh DM, Thomas LM, Karr EA. Crystal structure of a putative 3-hydroxypimelyl-CoA dehydrogenase, Hcd1, from *Syntrophus aciditrophicus* strain SB at 1.78 A resolution. *Acta Cryst F.* 2023;79(6).
- Thomas LM, Karr EA, Dinh DM. 3-oxoacyl-ACP reductase FabG. 2021; PDB ID 7SUB.

Preliminary Biochemical Characterization of FeSOR

An important but poorly understood process in syntrophic metabolism is how the electrons generated in the oxidation of acyl-CoA intermediates such as butyryl-CoA or glutaryl-CoA are used to produce hydrogen or formate. We identified a conduit of protein electron carriers involved in H_2 or formate production from the electrons generated in acyl-CoA oxidation in *Syntrophomonas wolfei* and *Syntrophus aciditrophicus*. The protein conduit includes acyl-CoA dehydrogenase, electron transfer flavoprotein AB, and a novel membrane-bound oxidoreductase (FeSOR). ***We hypothesized that FeSOR functions as an Etf:menaquinone oxidoreductase, which oxidizes Etf_{red} and reduces menaquinone in the membrane.*** We further **hypothesized** that electrons flowed from Etf_{red} to either FeS1* or FeS1 within the CCG domain of EMO, to FeS2, and finally to FeS3, before flowing to the hemes in the transmembrane region, and ultimately to 8-MMK (**Fig 4**). The iron-sulfur oxidoreductase, EMO, is the missing link connecting electrons obtained from fatty acid oxidation to the reduction of a menaquinone (8-MMK in *S. aciditrophicus*) in the membrane. The lack of genetic tractability of *S. aciditrophicus*

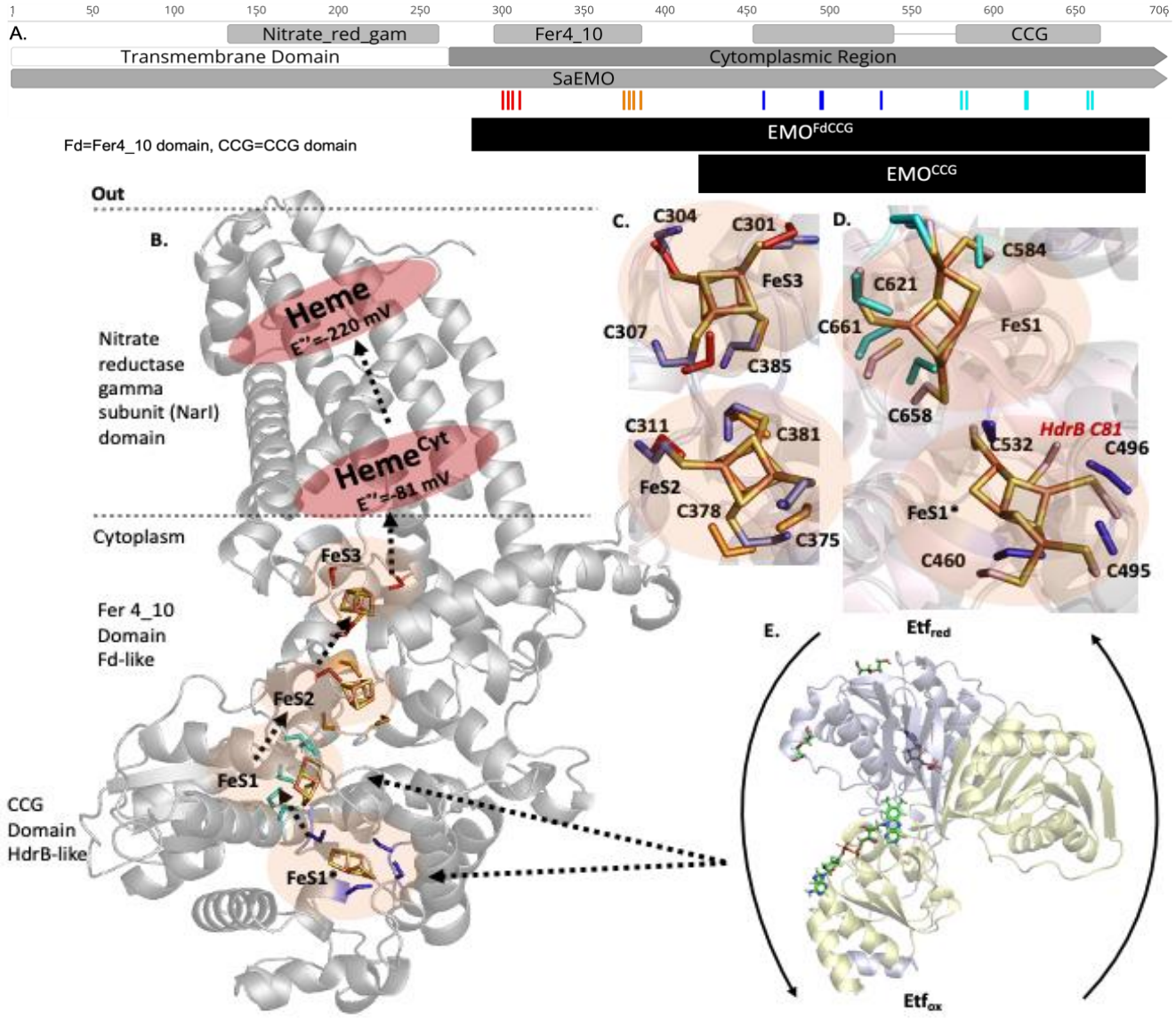

Figure 4. (A) Domain representation of *Sa*EMO with the transmembrane and cytoplasmic regions of the proteins indicated. Iron sulfur clusters in the ferredoxin domain are indicated in red and orange and those in the CCG domain are indicated in royal blue and cyan. The positions of N-terminal EMO truncations to be used in this study and their nomenclature are indicated. (B) The homology model of SaEMO with the domains indicated, the putative iron-sulfur clusters, and the numbering used. The iron-sulfur clusters from other structures (PDB IDs: 5ODH and 2FDN) are superimposed on the putative iron-sulfur clusters in *Sa*EMO for visualization. Cysteine side chains are displayed in the colors corresponding to the cysteine residues in A. Heme positions are based on the approximate positioning of the hemes in the NarI structure. (C) Zoomed region of *Sa*EMO ferredoxin domain overlayed with a bicluster 4Fe-4S ferredoxin (2FDN). *Sa*EMO cysteine residues are in red, and orange and the numbers correspond to those residues and not to 2FDN. (D). Zoomed region of *Sa*EMO CCG domain overlayed with a HdrB (5ODH). *Sa*EMO cysteine residues are in cyan (FeS1) and royal blue (FeS1*) and the numbers correspond to those residues and not to 5ODH. One exception is the notation of C81 from HdrB. (E). Crystal structure of *Sw*EtfAB3 at 2.5 Å solved in collaboration between Karr and Gunsalus research groups.

impairs interrogation of the role of the iron-sulfur clusters in electron flow through EMO.

The electrons are likely transferred along a conduit of iron-sulfur clusters in the cytoplasmic region of EMO to the high potential heme.

The EMO proteins from *S. aciditrophicus* (*Sa*) and *S. wolfei* (*Sw*) shared 43.2% identity and 59.6% similarity over the entire protein and contained three distinct domains (**Fig 4**). The cytoplasmic regions have slightly higher identity and similarity (50.3% identity, 65.5% similarity). Our proposed work sought to fill the remaining gaps in our understanding of the movement of electrons between Etf_{red} and the high-potential heme in the transmembrane domain. Further exploration of these hypotheses required heterologous expression of EMO to capitalize on the use of various protein truncations and/or amino acid substitutions to fully explore the role of the iron-sulfur clusters as an electron conduit. Full-length, truncated, and other variants of FeSOR homologues from *S. aciditrophicus* and *S. wolfei* were overexpressed in *Escherichia coli and Methanococcus maripaludis.* Despite significant attempts we were never successful in obtaining soluble protein with intact clusters from *E.coli* or *M. maripaludis* with any of our full-length or truncated constructs.

Structural characterization of *S. wolfei* EtfAB3

In collaboration with Drs. Rob Gunsalus and Mark Arbing at UCLA, we were able to crystallize and solved the structure of an electron transfer flavor protein from *S. woflei*, *Sw*EtfAB3, (*Sw* contains three EtfAB complexes compared to the one in *Sa*) (**Fig 4E**). However, *Sa*EtfAB only shares about ~30% identity/50% similarity to the *Sw*EtfAB3 complex. Resolved to 2.5 Å as a heterodimer, the structure of SwEtfAB3 maintains overall homology with Etf structures from many species, including a conserved β-FAD. Nevertheless, it was resolved with a novel ADP ligand instead of an α-FAD or AMP, which is consistently the case for Etf protein complexes. A key glycine residue proposed to be integral to flavin binding in electron bifurcating Etf complexes is missing in *Sw*EtfAB3.

- Yaghoubi S, Dinh DM, Thomas LM, Wofford NQ, McInerney MJ, Karr EA. Functional and Structural Characterization of AMP-forming Acetyl-CoA Synthetase (Acs1) from *Syntrophus aciditrophicus* strain SB. *Target journal: mBio.* In Preparation.
- Yaghoubi S. Biochemical insights into the unconventional approaches to energy conservation and electron transport in syntrophic metabolism. 2024; Dissertation – Doctor of Philosophy in Microbiology. https://shareok.org/handle/11244/340333.

Other projects

Thiosulfate disproportionation by *Desulfotomaculum thermobenzoicum*.

Desulfotomaculum thermobenzoicum grew by disproportionation of thiosulfate, forming stoichiometric amounts of sulfate and sulfide. *D. thermobenzoicum* initially oxidized thiosulfate to sulfate when hydrogen was added in levels exceeding those needed to stoichiometrically reduce thiosulfate to sulfide, indicating that thiosulfate transformation by disproportionating bacteria may be regulated by the relative abundance electron donor.

This was the first report of a gram-positive, thermophilic bacterium capable of obtaining energy for growth by thiosulfate disproportionation.

- Jackson BE, McInerney MJ. Thiosulfate disproportionation by *Desulfotomaculum thermobenzoicum*. *Appl Environ Microbiol.* 2000;66(8):3650-3653.
- Jackson BE. Bioenergetic Perspectives of Syntrophic Substrate Degradation. 1999; Dissertation - Doctor of Philosophy in Microbiology. https://shareok.org/handle/11244/5863.

Isolation and characterization of several new iron-reducing bacteria

Strains H-2, 172, TACP-2, and TACP-5 are non-motile, gram-negative, freshwater mesophilic strict anaerobes with a morphology identical to *Geobacter metallireducens* strain GS15^T. The 16S rRNA gene sequence analysis indicated these isolates belonged to the genus, *Geobacter*, in the delta subclass of the Proteobacteria. Significant differences in phenotypic characteristics, DNA-DNA homology and mol% G+C indicated that the four isolates represented three new species of the genus. The species were *Geobacter hydrogenophilus* (strain H-2^T), *Geobacter chapelleii* (strain 172 ^{T}), and *Geobacter grbicium* (strains TACP-2 and TACP-5).

- Coates JD, Bhupathiraju VK, Achenbach LA, McInerney MJ, Lovley DR. *Geobacter hydrogenophilus*, *Geobacter chapellei* and *Geobacter grbiciae*, three new, strictly anaerobic, dissimilatory Fe(III)-reducers. *International Journal of Systematic and Evolutionary Microbiology.* 2001;51:581-588.

Characterization of a new halophilc anaerobic bacterium.

Three strains, designated VS-751^T, VS-511 and VS-732, of a strictly anaerobic, moderately halophilic, gram-negative, rod-shaped bacterium were isolated from a highly saline (15-20%) brine oil reservoir in central Oklahoma. Despite the phenotypic differences among the three strains, analysis of the 16S rRNA gene sequences and DNA-DNA hybridizations showed that these three strains were members of the same species, of the genus *Haloanaerobium*. We proposed that strain VS-751^T (ATCC 700103) be established as *Haloanaerobium kushneri*.

- Bhupathiraju VK, McInerney MJ, Woese CR, Tanner RS. *Haloanaerobium kushneri* sp nov., an obligately halophilic, anaerobic bacterium from an oil brine. *International Journal of Systematic Bacteriology.* 1999;49:953-960.

Anaerobic metabolism and its regulation

Sediments from a hydrocarbon-contaminated aquifer, where periodic shifts between sulfate reduction and methanogenesis occurred, were examined to determine whether the degradation of toluene under sulfate-reducing conditions depended on interspecies hydrogen transfer. Toluene degradation under sulfate-reducing conditions was inhibited by the addition of 5 mM sodium molybdate, but the activity was not restored upon the addition of an actively growing, hydrogen-using methanogen. Toluene degradation was not inhibited in microcosms where hydrogen levels were maintained at a level

theoretically sufficient to inhibit toluene degradation if the process proceeded via interspecies hydrogen transfer. Finally, the addition of carbon monoxide, a potent inhibitor of hydrogenase activity, inhibited hydrogen but not toluene consumption in sulfate-reducing microcosms. These results suggest that toluene is degraded directly by sulfate-reducing bacteria without the involvement of interspecies hydrogen transfer.

- Elshahed MS, McInerney MJ. Is interspecies hydrogen transfer needed for toluene degradation under sulfate-reducing conditions? *Fems Microbiology Ecology.* 2001;35(2):163-169.

Microbial physiology in undergraduate teaching

We developed a novel approach to teaching undergraduate microbial metabolism/physiology called team-based learning. Team-based learning improved the comprehension and critical thinking of students and resulted in high learning intensity. Team-based learning with the inclusion of challenging projects also improved student attitudes about the course and altered student-instructor interactions (focused on learning rather than grades.

- McInerney MJ, Fink LD. Team-based learning enhances long-term retention and critical thinking in an undergraduate microbial physiology course. *Microbiology Education.* 2003;4:3-12.

Microbial community involved in acetate and butyrate degradation in a gas condensate-contaminated aquifer.

The anaerobic metabolism of acetate and butyrate was studied in sediments from a gas condensate-contaminated aquifer where sulfate is the predominate electron acceptor. The production of ^{14}C-methane from 2-^{14}C-acetate and the presence of bands with sequence similarity to *Methanosaetaceae* in acetate enrichments with and without sulfate as detected by denaturing gradient gel electrophoresis (DGGE) shows that acetoclastic methanogenesis is the dominant fate of acetate in these sediments. Most probable number analysis showed that a similar number of butyrate degraders were present in tubes with butyrate and sulfate, butyrate, sulfate and a hydrogen-using sulfate reducer, and butyrate without sulfate but with a hydrogen-using methanogen. DGGE of the butyrate enrichments with sulfate with or without the hydrogen user showed an identical predominant band that had sequence similarity to members of the genus *Syntrophus*. Sequence analysis of 100 clones indicated that members of the genus *Syntrophomonas* were present in all enrichment and accounted for about 30% of the total sequences. Members of the genus *Desulfovibrio* accounted for 75% of the sequences representing sulfate-reducing bacteria in enrichments with butyrate and sulfate. The presence of sequences similar to syntrophic bacteria in butyrate enrichments with sulfate suggests that syntrophic butyrate metabolism may be an essential process even in environments where sulfate is the predominant electron acceptor.

Biological Cr(VI) reduction was studied in anaerobic sediments from an aquifer in Norman, Okla. Microcosms containing sediment and mineral medium were amended with various electron donors to determine those most important for biological Cr(VI) reduction. Cr(VI) (about 340 μM) was reduced with endogenous substrates (no donor), or acetate was added. The addition of formate, hydrogen, and glucose stimulated Cr(VI) reduction compared with reduction in unamended controls. From these sediments, an anaerobic Cr(VI)-utilizing enrichment was obtained that was dependent upon hydrogen for both growth and Cr(VI) reduction. No methane was produced by the enrichment, which reduced about 750 μM Cr(VI) in less than six days. The dissolved hydrogen concentration was used as an indicator of the terminal electron accepting process occurring in the sediments. Microcosms with sediments, groundwater, and chromate metabolized hydrogen to a concentration below the detection limits of the mercury vapor gas chromatograph. In microcosms without chromate, the hydrogen concentration was about 8 nM, a concentration comparable to that under methanogenic conditions. When these microcosms were amended with 500 μM Cr(VI), the dissolved hydrogen concentration quickly fell below the detection limits. These results showed that the hydrogen concentration under chromate-reducing conditions became very low, as low as that reported under nitrate- and manganese-reducing conditions, a result consistent with the free energy changes for these reactions. The utilization of formate, lactate, hydrogen, and glucose as electron donors for Cr(VI) reduction indicates that increasing the availability of hydrogen results in a greater capacity for Cr(VI) reduction. This conclusion is supported by the existence of an enrichment dependent upon hydrogen for growth and Cr(VI) reduction.

- Marsh T, Leon N, McInerney M. Physiochemical factors affecting chromate reduction by aquifer materials. *Geomicrobiology Journal.* 2000;17(4):291-303.
- Marsh T, McInerney M. Relationship of hydrogen bioavailability to chromate reduction in aquifer sediments. *Appl Environ Microbiol.* 2001;67(4):1517-1521.
- Struchtemeyer C, Elshahed M, Duncan K, McInerney M. Evidence for aceticlastic methanogenesis in the presence of sulfate in a gas condensate-contaminated aquifer. *Appl Environ Microbiol.* 2005;71(9):5348-5353.
- Struchtemeyer CG. Microorganisms from Anaerobic, Gas Condensate-Contaminated Sediments that Degrade Acetate, Butyrate, and Propionate Under Methanogenic and Sulfate-reducing Conditions. 2009; Dissertation - Doctor of Philosophy in Microbiology. https://shareok.org/handle/11244/319156.
- Struchtemeyer CG, Duncan KE, McInerney MJ. Evidence for syntrophic butyrate metabolism under sulfate-reducing conditions in a hydrocarbon-contaminated aquifer. *Fems Microbiology Ecology.* 2011;76(2):289-300.

Progress curve analysis

We developed a simple method to estimate kinetic parameters from progress curve data that can be reduced to forms analogous to the Michaelis-Menton equation. The Lambert *W* function allows an explicit, closed-form solution to differential rate

expressions that describe the dynamics of substrate decay. The applicability of this approach was verified by using data sets where normally distributed noise of known mean and standard deviation was added to synthetic data to mimic common experimental data sets. Also, experimental data consisting of hydrogen depletion in activated sludge was also used to test the approach.

- Goudar CT, Harris SK, McInerney MJ, Suflita JM. Progress curve analysis for enzyme and microbial kinetic reactions using explicit solutions based on the Lambert *W* function. *Journal of Microbiological Methods.* 2004;59(3):317-326.

Role of cytochrome c_3 of *Desulfovibrio vulgaris*

Respiratory assays and reduced minus oxidized spectra of the wild-type strain and mutants defective in the Fe-only hydrogenase and the membrane-bound high molecular weight cytochrome *c* complex were carried out to determine *c*-type cytochrome involvement in metal and sulfate reduction. Interestingly, we did not find evidence for the involvement of cytochrome c_3 in hydrogen-mediated sulfate reduction but did show its role in the reduction of iron and uranium.

We found that cytochrome c_3 of *Desulfovibrio vulgaris* is involved in hydrogen-mediated metal reduction, but it is not involved in hydrogen-mediated sulfate reduction. We have developed a simple method to estimate kinetic parameters from progress curve analyses of biologically catalyzed reactions. The Lambert W function is used to obtain explicit, closed-form solutions to differential rate expressions that describe substrate depletion dynamics. Finally, we have found a novel growth factor requirement for certain *Bacillus* species. Strains of *Bacillus subtilis* and *Bacillus mojavensis* require DNA or a mixture of four deoxyribonucleotides for anaerobic growth.

- Elias DA, Suflita JM, McInerney MJ, Krumholz LR. Periplasmic cytochrome c(3) of *Desulfovibrio vulgaris* is directly involved in H-2-mediated metal but not sulfate reduction. *Appl Environ Microbiol.* 2004;70(1):413-420.

Anaerobic growth of *Bacillus mojavensis* requires DNA

Bacillus mojavensis strain JF-2 and three other *Bacillus* strains require four deoxyribonucleosides or DNA for growth under strictly anaerobic conditions. These growth factors were not required for aerobic growth. The addition of five nucleic acid bases, four ribonucleotides or four ribonucleosides did not replace the requirement for four deoxyribonucleosides. The addition of salmon sperm DNA, herring sperm DNA, *Escherichia coli* DNA and synthetic DNA (single- or double-stranded) allowed anaerobic growth. This work provides strong evidence that externally supplied deoxyribonucleosides can be used to maintain a balanced deoxyribonucleotide pool for DNA synthesis and suggests that ribonucleotide reductases are not essential to the bacterial cell cycle nor are they necessarily part of a minimal bacterial genome.

- Folmsbee M, McInerney M, Nagle D. Anaerobic growth of *Bacillus mojavensis* and *Bacillus subtilis* requires deoxyribonucleosides or DNA. *Appl Environ Microbiol.* 2004;70(9):5252-5257.

- Folmsbee M, Duncan K, Han SO, Nagle D, Jennings E, McInerney M. Re-identification of the halotolerant, biosurfactant-producing *Bacillus licheniformis* strain JF-2 as *Bacillus mojavensis* strain JF-2. *Syst Appl Microbiol.* 2006;29(8):645-649.

Odor control of swine waste

Odor control and disposal of swine waste has inhibited the expansion of swine production facilities throughout the US. Swine waste odor is primarily associated with the high concentrations of branched and straight chain volatile fatty acids (VFAs). We demonstrated that a stimulated iron biogeochemical cycle in hog manure can rapidly remove the odiferous compounds and enhance methane production 200%. When raw waste was amended with Fe(III) and an Fe(III)-reducing bacterium, the VFA content rapidly decreased corresponding with an almost complete removal of the odor. In contrast, the VFA content of the raw waste without iron or inoculation showed a marked increase in VFA content and a rapid pH drop. This study showed that Fe(III) supplementation combined with appropriate bioaugmentation provides a simple, cost effective approach to deodorize and treat swine waste, which removes a significant impediment to the expansion of pork production facilities allowing them to benefit from economies of scale.

- Coates JD, Cole KA, Michaelidou U, Patrick J, McInerney MJ, Achenbach LA. Biological control of hog waste odor through stimulated microbial Fe(III) reduction. *Appl Environ Microbiol.* 2005;71(8):4728-4735.

Anaerobic metabolism of aklylbenzenes

We studied the anaerobic metabolism of alkylbenzenes and detected signature metabolites that attest to the *in situ* anaerobic attenuation of alkylbenzenes. An accurate assessment of the fate of hydrocarbons spilled in aquifers is essential for gauging associated health and ecological risks. Regulatory pressure to actively remediate such contaminated ecosystems can be substantially diminished if solid evidence for *in situ* microbial destruction of pollutants is obtained. In laboratory incubations, sediment-associated microorganisms from a gas condensate-contaminated aquifer anaerobically biodegraded toluene, ethylbenzene, and xylene and toluic acid isomers with stoichiometric amounts of sulfate consumed or methane produced. The activation of the alkylated aromatic contaminants involved conversion to their corresponding benzylsuccinic acid derivatives, a reaction known to occur for toluene and *m*-xylene decay but one previously unrecognized for ethylbenzene, *o*- and *p*-xylene, and *m*-toluate metabolism. Benzylsuccinates were further biodegraded to toluates, phthalates, and benzoate. During meta-toluate degradation under methanogenic conditions, meta-carboxybenzylsuccinate accumulated, indicating that the addition reaction is also used for the activation and subsequent degradation of carboxylated aromatic compounds. Several of these metabolites, which transiently accumulated during laboratory incubations, were also detected in groundwater samples from the aquifer where alkylbenzene concentrations had decreased over time, providing evidence that anaerobic microbial metabolism of these contaminants occurs *in situ.* Our studies confirm the utility of the aforementioned compounds as signature metabolites attesting to the natural attenuation of aromatic hydrocarbons in anaerobic environments.

- Elshahed MS, Gieg LM, McInerney MJ, Suflita JM. Signature metabolites attesting to the *in-situ* attenuation of alkylbenzenes in anaerobic environments. *Environmental Science & Technology.* 2001;35(4):682-689.